Observation of microseconds-order non-uniform intra electron bunch train photoemission from the cesium-telluride photocathode

Contents

- Experimental observation
- Surface states and band bending
- Surface effects
- Cathode work function and overall QE modeling
- Simulation results
- Explanations for Q-train experiments

Ye Chen, 06.2018

Experimental results

Cathode driven laser

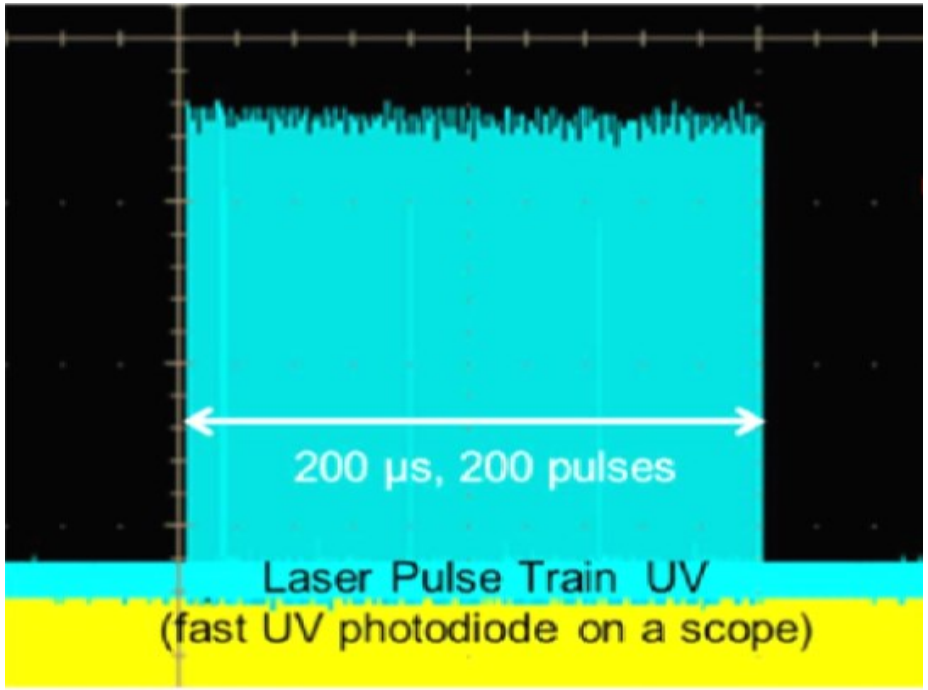

Charge measured at gun exit

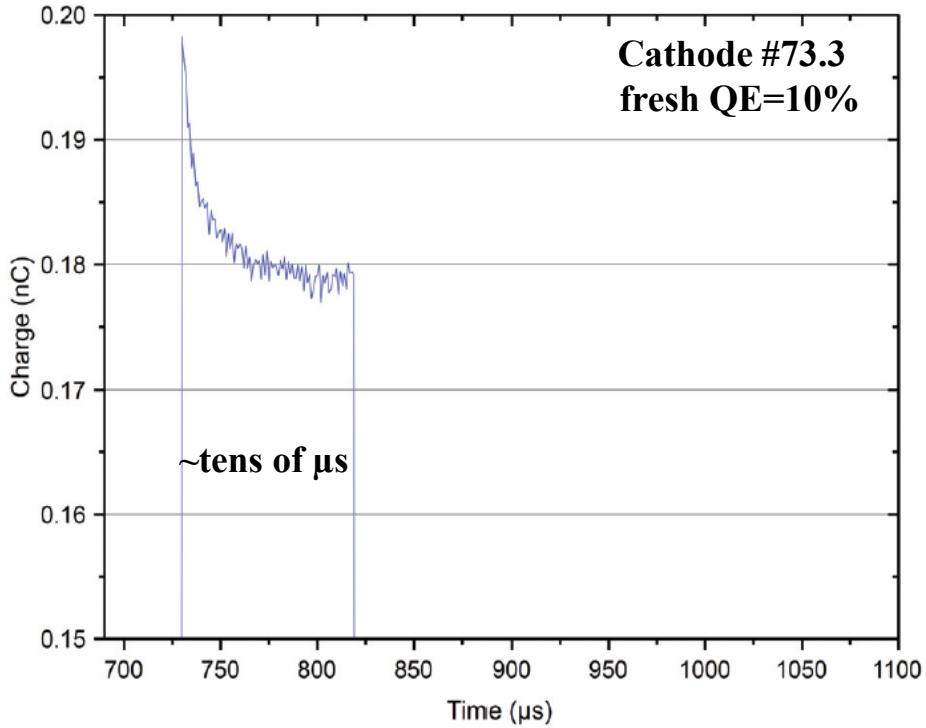

- A flat energy distribution of the laser pulse train produces a "spike" at the head of the electron bunch train emitted from a "fresh" cathode
- The spike depends on laser energy density and accelerating field on cathode
- The spike "vanishes" over long operation time (months)

Experimental results

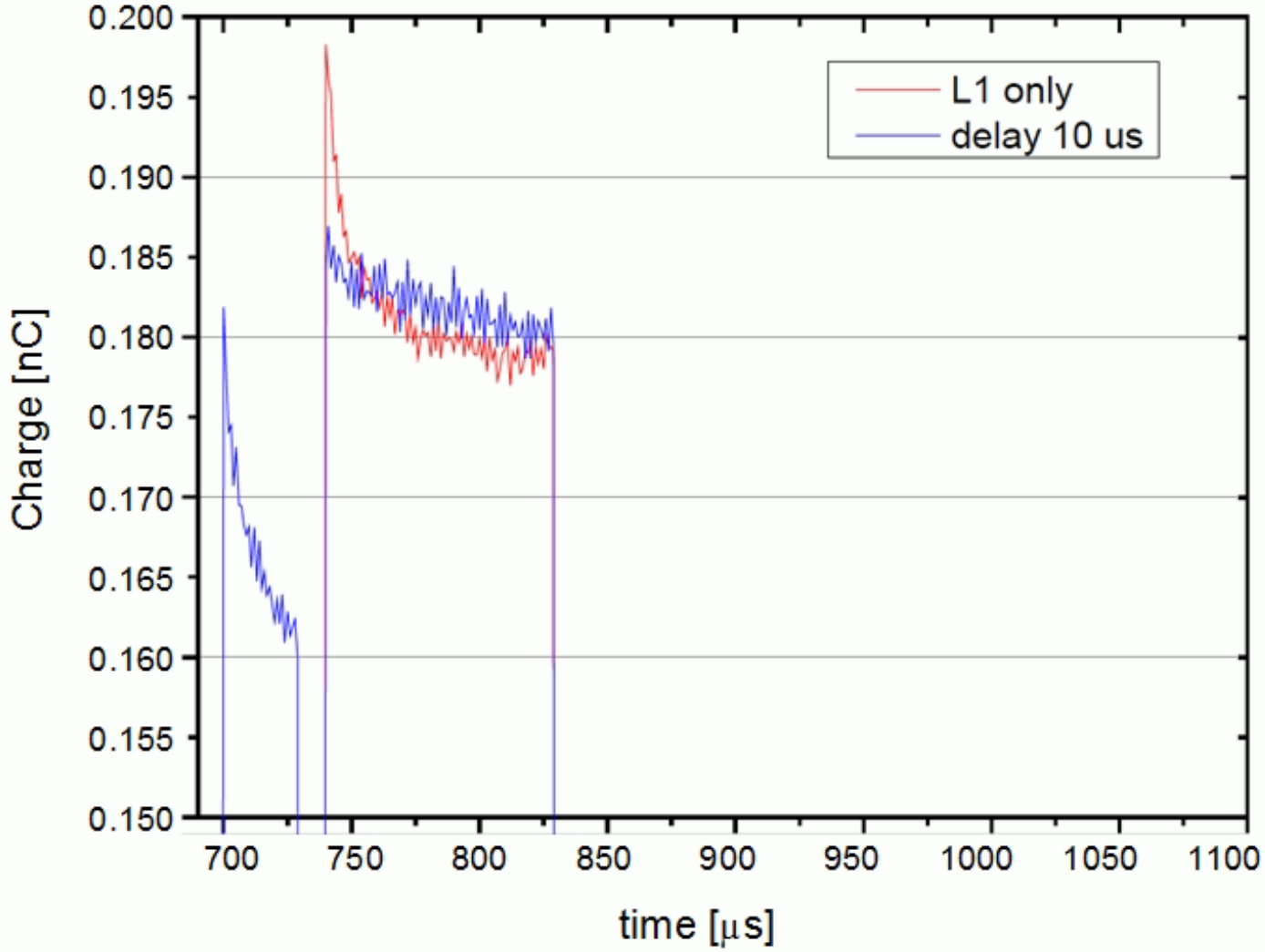

Conclusive thoughts from experiments

From 17.02.2015

- The spike in the charge distribution is **real**:
  - Visible on all charge measurement devices
  - Visible also on the BAM and BCMs
- The spike in the charge distribution originates from the **cathode**.
- After **~30 µs** the charge distribution is flat
  - Whatever at the cathode happens takes extremely long in terms of **surface physics**
- The effect of the spike is charge or **laser energy density dependent**
  - At low densities the spikes disappears
- The effect of the spike is **field dependent**
  - At low fields the spike disappears

Surface states

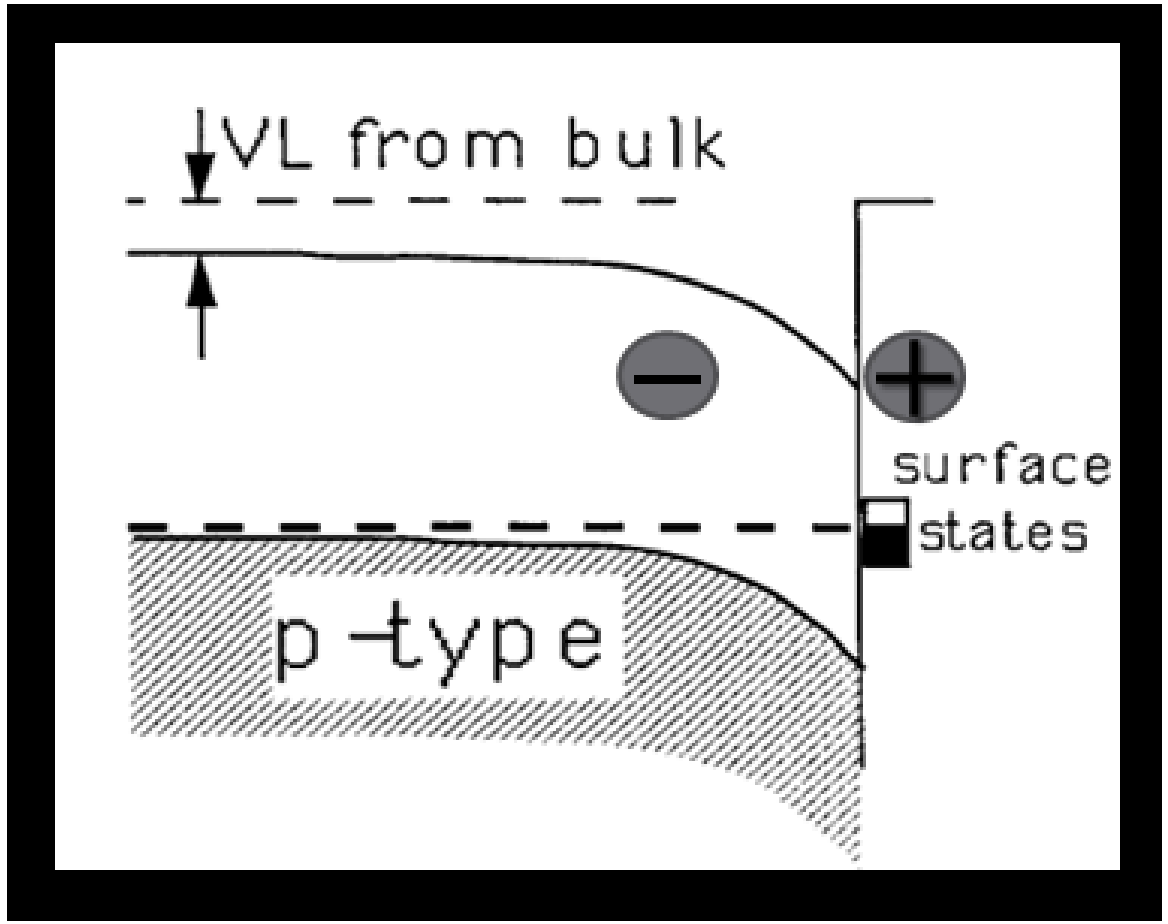

Schematic band structure for a p-type semiconductor

- Finite (long) semiconductor

  → **surface states naturally exist**

- Surface states have typical **energies inside the band gap**
- The band has to be bent to match the chemical potential in the bulk ("Fermi level") with that on the surface

Band (surface) bending potential

Band structure

- Cs_2Te: p-type semiconductor
- p-type: the **band bent downwards**
- The surface vacuum level decreases w.r.t. the bulk CBM
- The effective barrier seen by the electrons in the bulk is smaller than in the flat band case

→ **Emission enhanced w.r.t. flat band case**

- For p-type, **the holes occupy the donor-like surface states**
- Positive surface charge produced, counterbalanced effectively by ionized charges in the depletion layer near the surface

Surface effects

- **Existing holes on the surface**
  →large population (depends on doping concentration)
  →long living time (hundreds of microseconds possible)
- **Change of surface bending potential**
  →extracted electrons combine with holes on surface
  →this can change the local charge equilibrium, and therefore, the surface potential
  →surface potential change affects the vacuum level seen by the extracted electrons

→ Both effects have impacts on the effective cathode QE:
  → direct consuming extracted electrons or by changing the surface bending potential
→ The impacts of these surface effects are reflected by the cathode work function

Effective QE modeling

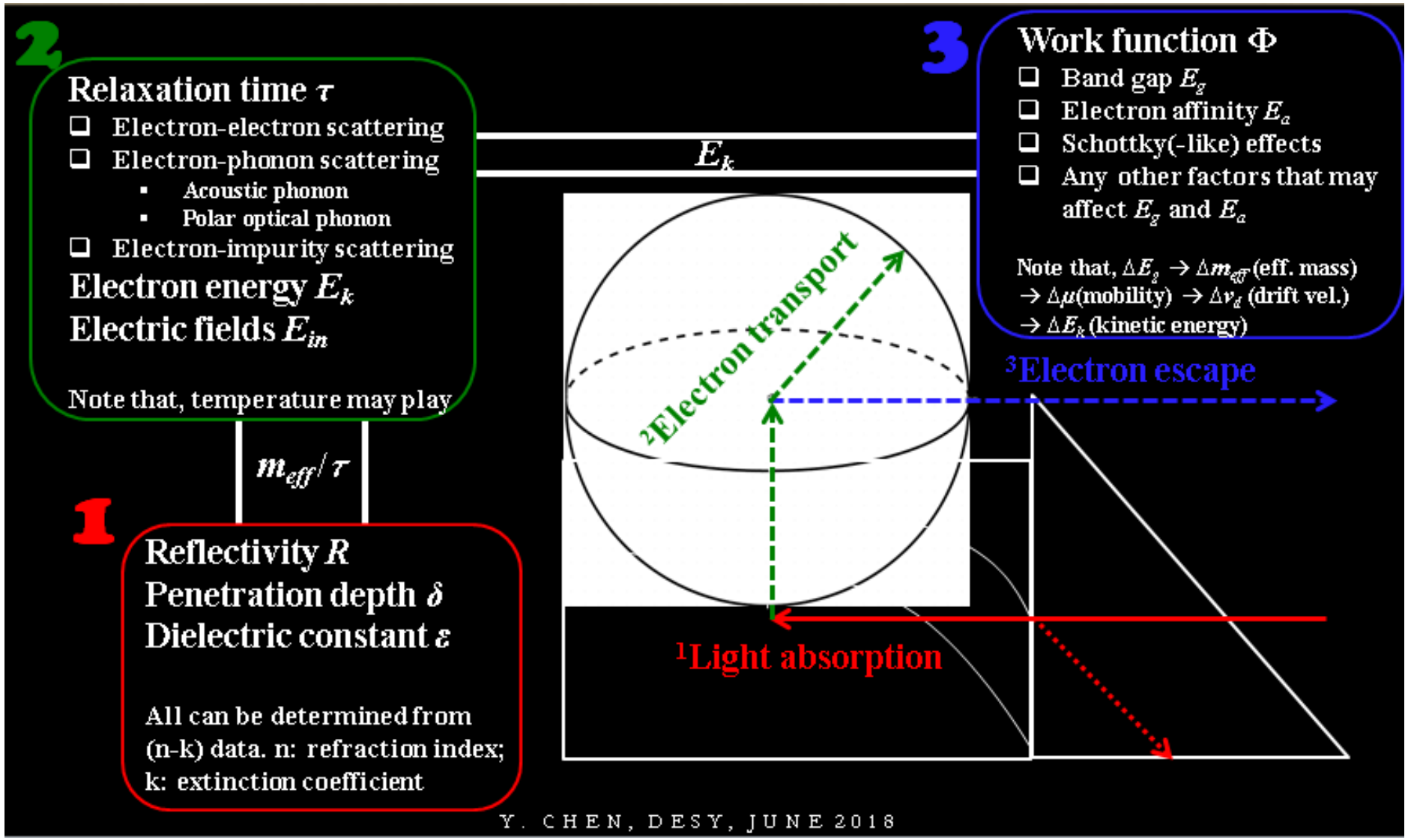

Reflection and penetration

- Complex refraction coefficient of materials: $\hat{n} = n + ik$
- **Data from dispersive analysis: λ ∈[250 517]nm; n ∈ [0.8 1.8]; k ∈ [0.3 0.7];**

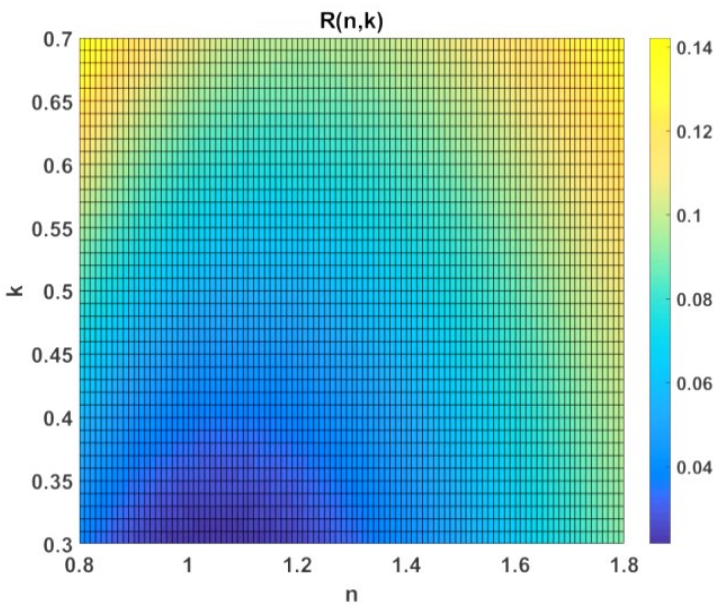

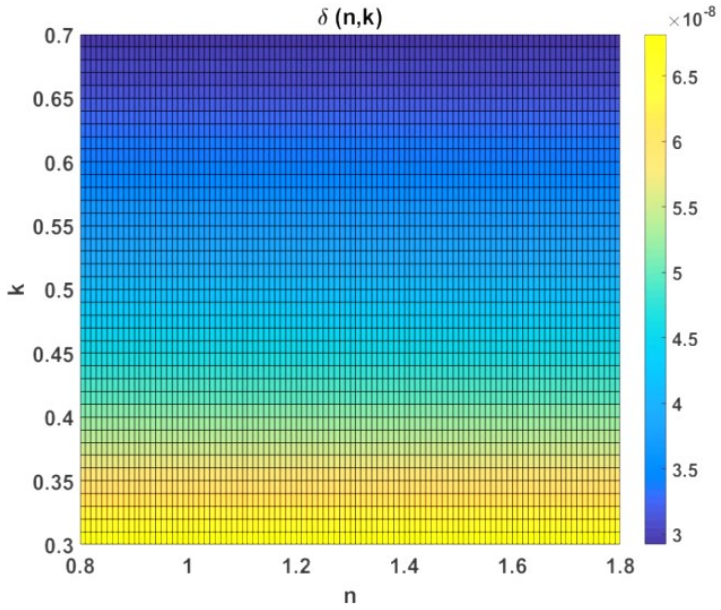

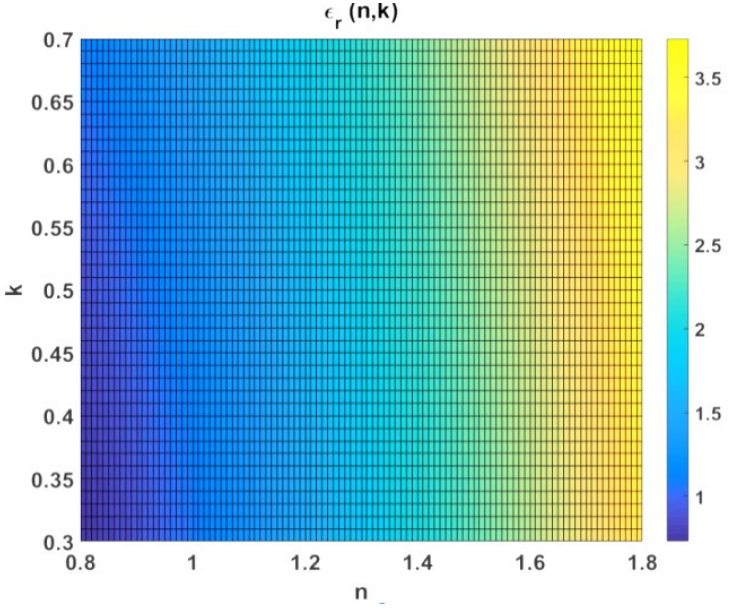

Reflectivity, $R \approx \frac{(n-1)^2+k^2}{(n+1)^2+k^2}$

Penetration depth, $\delta \approx \frac{\lambda}{4\pi k}$

Dielectric constant, $\varepsilon_r \approx (n-ik)^2$

→ @ λ = 257 nm, take $\delta(\omega) \approx 50$ nm, $R(\omega) \approx 2\%$ into the contributions to the overall QE

Calculated Cs_2Te specified band properties

for modeling scattering effect

Physical Property	Calculation for Cs_2Te		Cross-Refs to Cs_3Sb
Mass density	$\rho = \frac{4(2M_{Cs} + 1M_{Te})}{\Delta V} \approx \mathbf{3.99\ g/cm^3}$	1	4.519 g/cm^3
Sound velocity	$v_s = \sqrt{\frac{c_{11}}{\rho}} \approx \mathbf{5484\, m/s}$	2	5153 m/s
Phonon energy (lowest mode)	$\hbar\omega_q = \frac{4\pi\hbar v_s}{\lambda_{pm}} \approx \mathbf{0.0767 eV}$		0.05 eV
Average ionic radii	$l \approx \mathbf{0.194\ nm}$	3	0.14 nm
Deformation potential	$\Xi = Dl \approx 9.7$ eV	4	7 eV
Bloch–Grüneisen function	$W_-\left(5, \frac{\Theta}{T}\right) \approx (\frac{\Theta}{T})^4/4$		
Fine structure coefficient	$\alpha_{fs} = e^2/4\pi\epsilon_0\hbar c \approx 1/137.1$		
Effective mass	$m = \frac{E_g}{E_{Ry}} m_0 \approx \mathbf{0.24\ m_0}$		0.1176 m_0

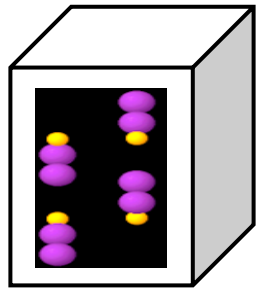

Unit cell of Cs_2Te

1. Thermal expansion not considered
2. Generic elastic constant, c_{11} = 12×10^{10} N/m^2
3. Average of the ionic radii of Cs and Te
4. Mean deformation potential constant D = 5×10^8 eV/cm

Scattering effects

- Electron-electron scattering → **dominating for metal cathodes**

- **Electron-phonon scattering → dominating for semiconductor cathodes**
  - ✓ **Polar optical phonon** (vibration within a cell, v_g=0, standing…)
  - ✓ **Acoustic phonon (**vibration of a cell, v_g>0, travelling…**)**

- Electron-impurity(defect) scattering
  → **presumably much weaker effect than others for normal doping concentration**

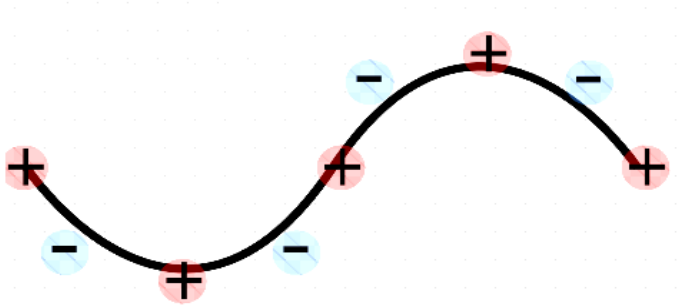

Acoustic phonon mode

Optical phonon mode

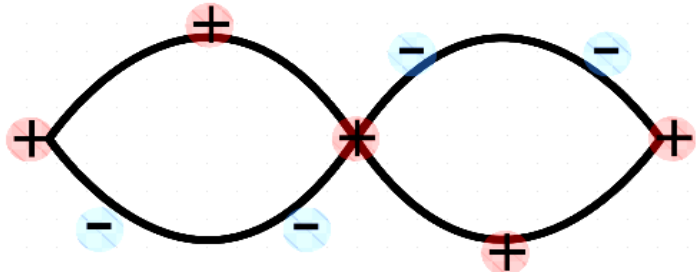

Optical phonon scattering, τ_{pop}

$$\frac{1}{\tau_{pop}} = 2\omega_q \Delta\epsilon \left[2 \frac{1}{\exp\left(\frac{\hbar \boldsymbol{\omega_q}}{k_B T}\right) - 1} + 1 \right] \frac{16u^2 + 18u + 3}{3(1+2u)\sqrt{u(u+1)}}$$

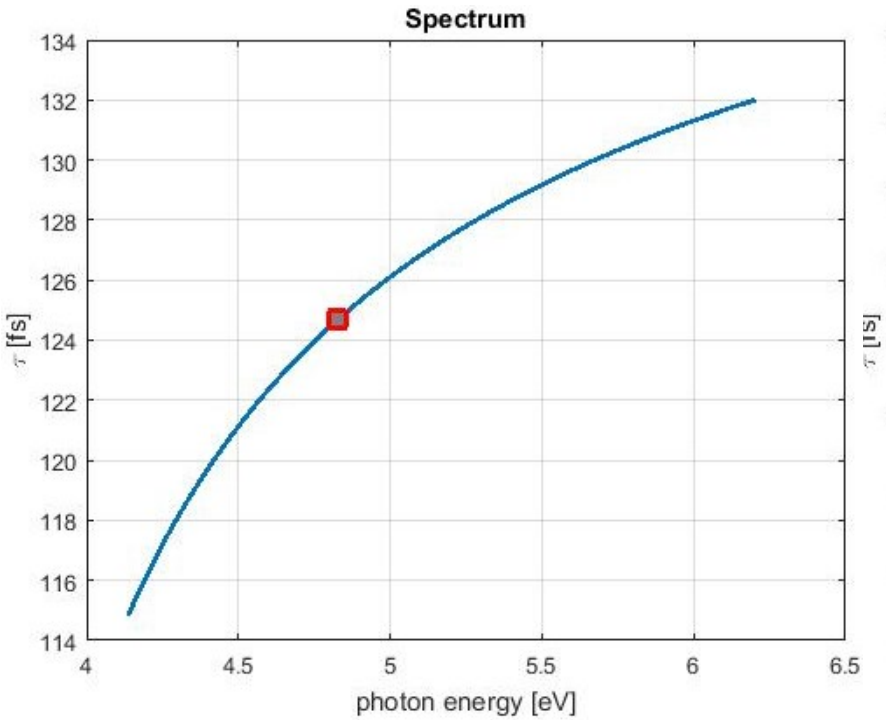

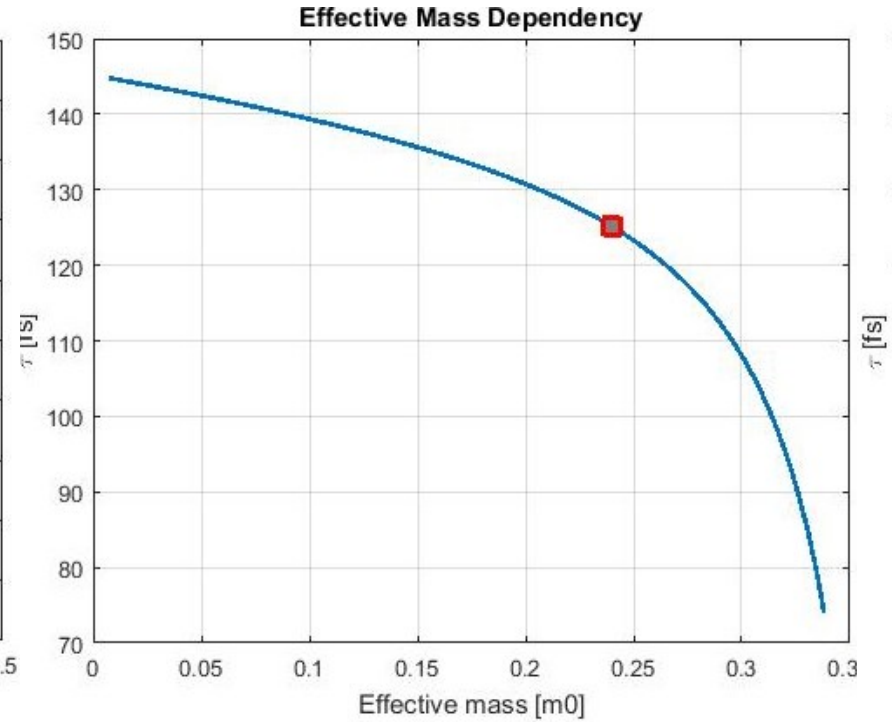

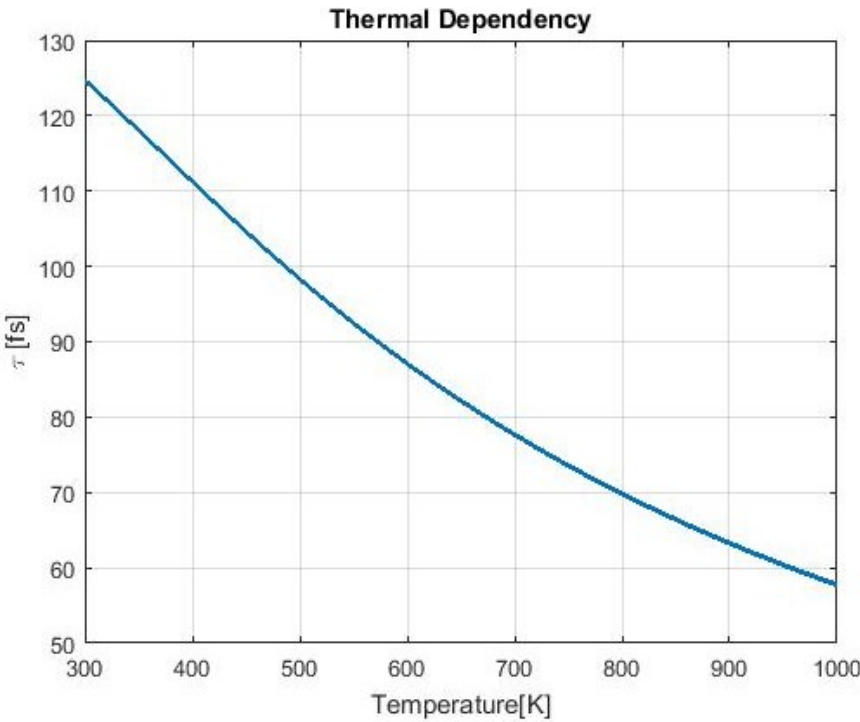

Contribution to overall QE

Taking weighted scattering fraction function as
("the fraction of electrons surviving from the scattering effects weighted by escape angles in a 3D half emission sphere)

$$F = p^2 log\left[\frac{x(1+p)}{1+xp}\right] + \frac{1}{2x^2}(1-x)(2xp-x-1)$$

where $1/x$ characterizes cosine of the escape cone angle, p stands for the ratio of the penetration depth δ obtained from the first step to the eff. distance l between scattering events in the second step, where l is calculated using the scattering rate obtained from the second step and the electron energy which is determined from the photon energy and the eff. cath. work function with the objective to fit the measured cath. eff. QE in later calculations.

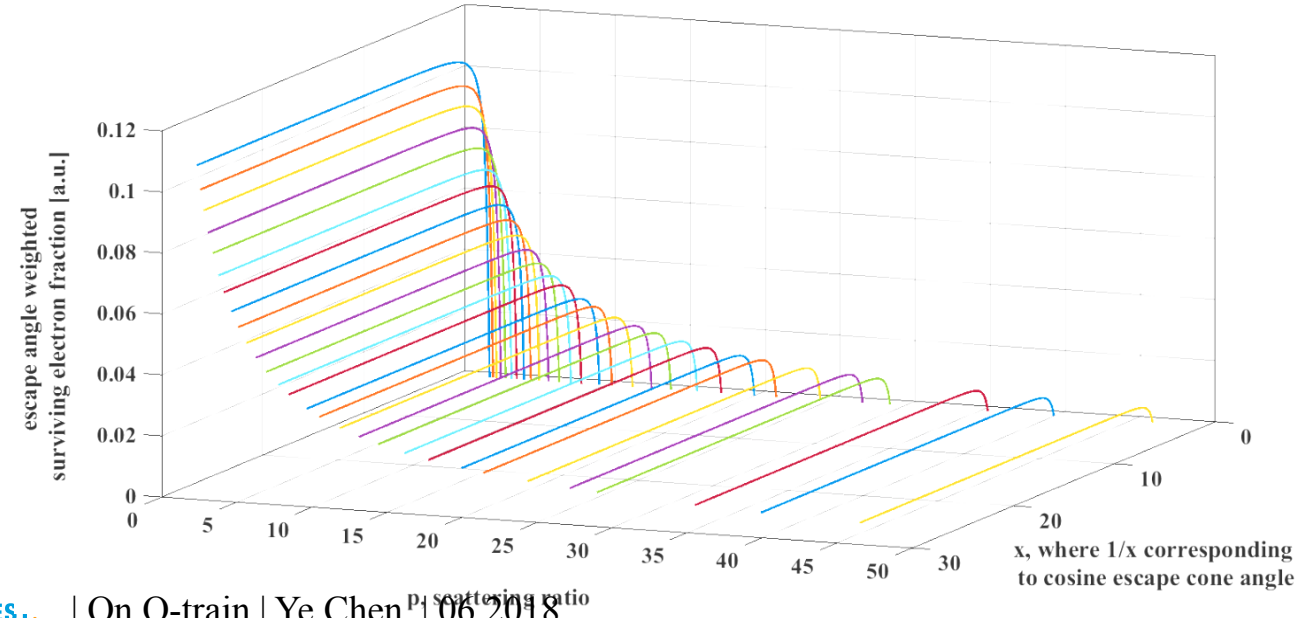

- Larger l gives smaller p for a given δ
- Smaller p physically interpreting larger distance / time interval between scattering events → higher escape probability, larger fraction of surviving electrons

Cathode work function and the overall QE

Define, $\boldsymbol{\Phi_w = E_g + E_a + dE_{band} - dE_{schottky}}$

where E_g, dE_{band} and $dE_{schottky}$ represent the band gap, band bending potential variation induced and Schottky-effect induced work function corrections, respectively.

with $dE_{schottky} \propto \sqrt{\frac{q^3 E_{RF}}{4\pi\epsilon_0}}$ and

dE_{band}: correction term of the cath. work function due to band bending potential modification

$$\mathbf{QE} = \frac{(\mathbf{1}-\boldsymbol{R})}{\mathbf{2}}\boldsymbol{G}\left\{\sqrt{\mathbf{1}+\frac{\hbar\boldsymbol{\omega}-\boldsymbol{\Phi_w}}{\boldsymbol{E_a}}}\right\} \approx \frac{(\mathbf{1}-\boldsymbol{R})}{\mathbf{2}(\boldsymbol{p_0}+\mathbf{1})(\mathbf{1}+\frac{\boldsymbol{E_a}}{\hbar\boldsymbol{\omega}-\boldsymbol{\Phi_w}})^2} \qquad \boldsymbol{G_\lambda(y)} = \frac{\mathbf{4}(\mathbf{1}-\boldsymbol{R})}{\boldsymbol{y^4}}\int_1^y \boldsymbol{x^3 F_\lambda(x)dx}$$

where

$\Phi_w = E_g + E_a + dE_{band} - dE_{schottky}$ with $dE_{schottky} = \sqrt{\frac{q^3 E_{RF}}{4\pi\epsilon_0}}$

R represents the reflection coefficient

An example for explaining the Q-train measurements

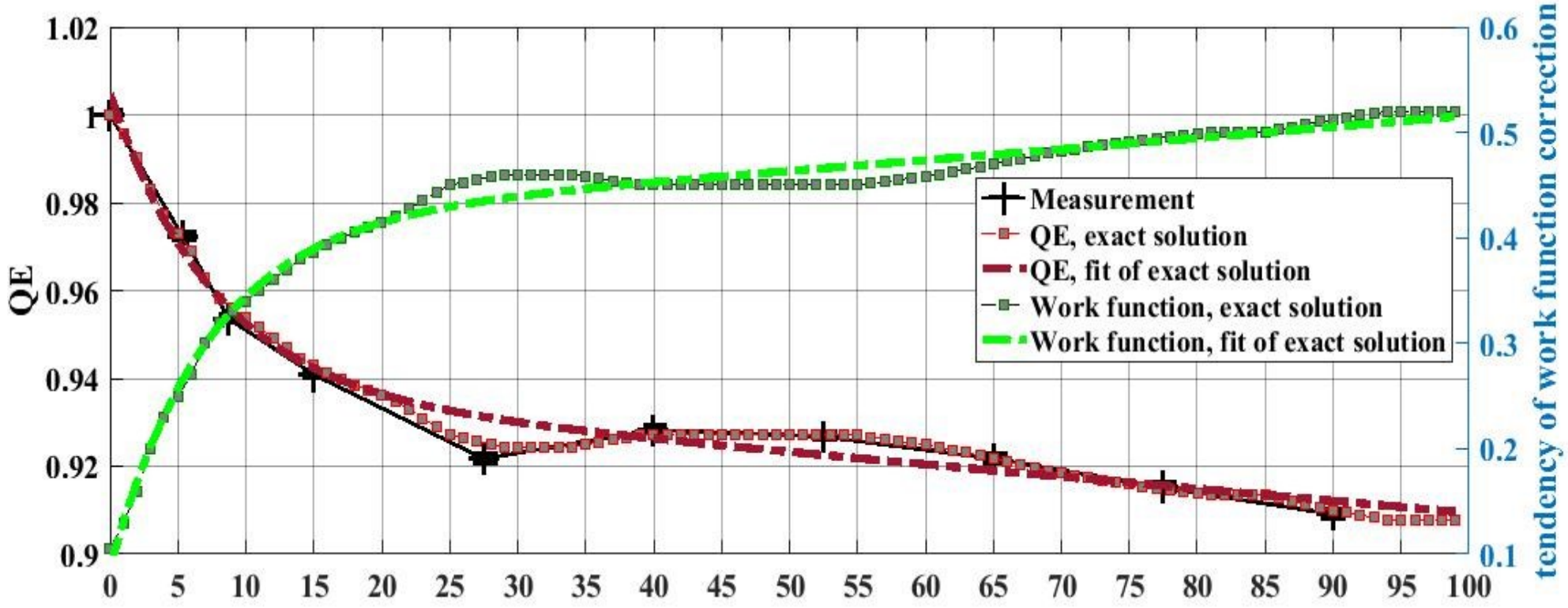

✓ Implementation of a correction term in the cath. eff. work function (e.g., up to 0.5 eV in this case) results in rather a good agreement of the QE decaying tendency between measurement and simulation

Backups: explaining more measurements

- **Case A → L1 and L2 on cath., L1 intensity —, L2 intensity↑, L1-L2 delay=0**
- **Case B → L1 and L2 on cath., L1 intensity —, L2 intensity↑, L1-L2 delay=0**
- **Case C → L1 and L2 on cath., L1 intensity —, L2 intensity↑, L1-L2 delay=0**
- **Case D → L1 on cath., w/ RF; L2 off, w/o RF**
- **Case E → L1 on cath., w/ RF; L2 on cath., w/o RF**
- **Case F → L1 on cath., w/ RF; L2 on cath., w/ RF and w/o RF**
- **Case G → L1 and L2 on cath., w/ RF, RF power level adjusted**
- **Case H → L1 and L2 on cath., w/ low RF power 1.28 MW, L2 intensity adjusted**
- **Case I → L1 and L2 on cath., w/ RF, L1-L2 delay adjusted**

A. L1 and L2 both on cathode, keep L1 intensity, increase L2 intensity step by step

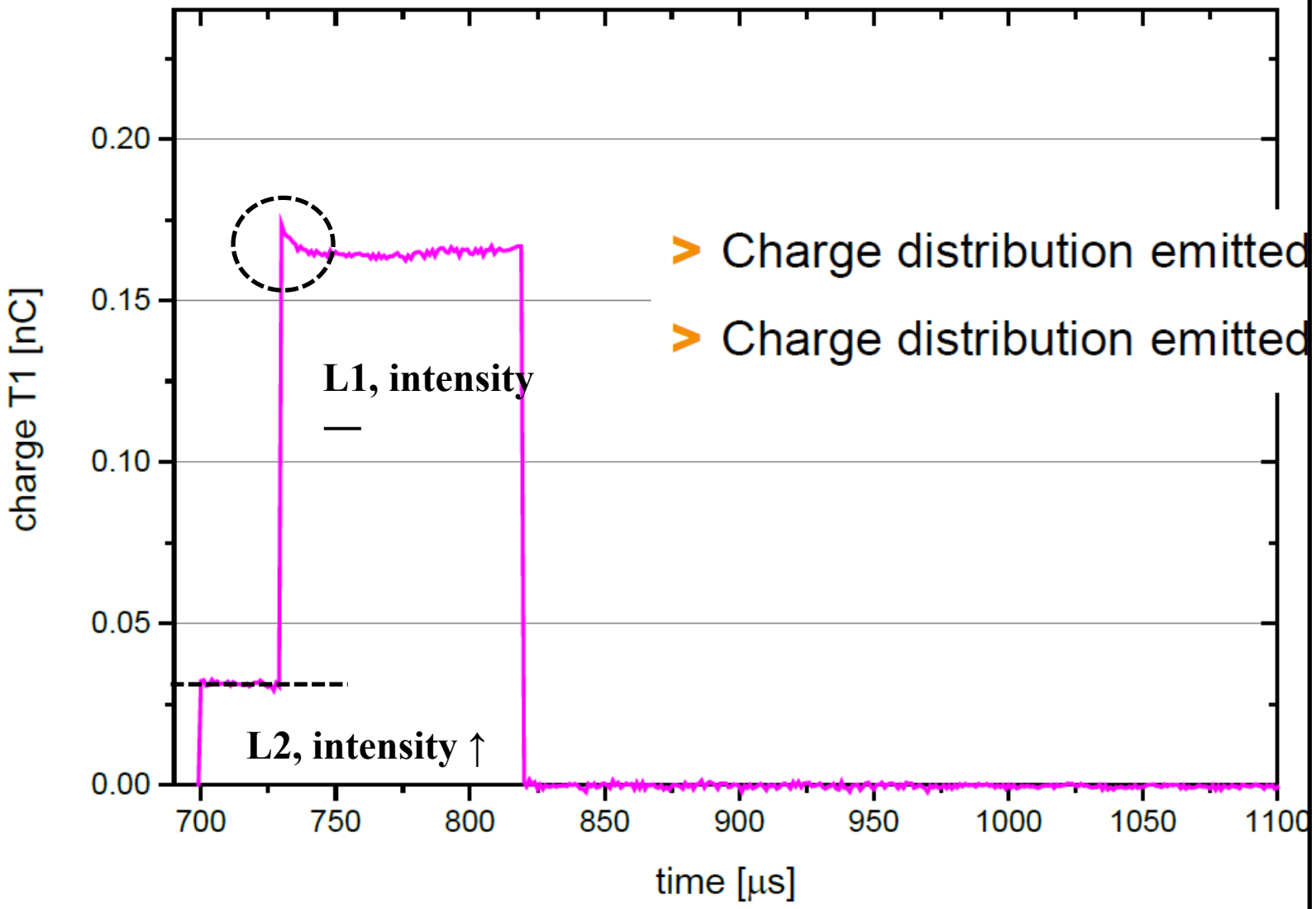

1. **Cath. eff. QE not varied during L2 illumination**
   a. Low intensity L2 not able to produce sufficient number of living electrons on the cath. surface
   b. Local band bending potential not significantly modified
   c. Cath. work function thus not changed, i.e., the cath. eff. QE not changed
2. **Higher intensity L1 producing much more electrons per µs on the cath. surface, plus, electron pre accumulation during L2 illumination on the surface, resulting in**
   a. Local charge distribution at the cath. surface changed, thus the local band bending potential modified
   b. Work function dynamically modified (ΔΦ↑→ QE↓) along the L1 train until the consumption of surface holes compensated by dopant supplements (to keep bending potential dynamically invariant), where a flat QE (i.e., flat Q-train) can be rendered

B. L1 and L2 both on cathode, keep L1 intensity, increase L2 intensity step by step

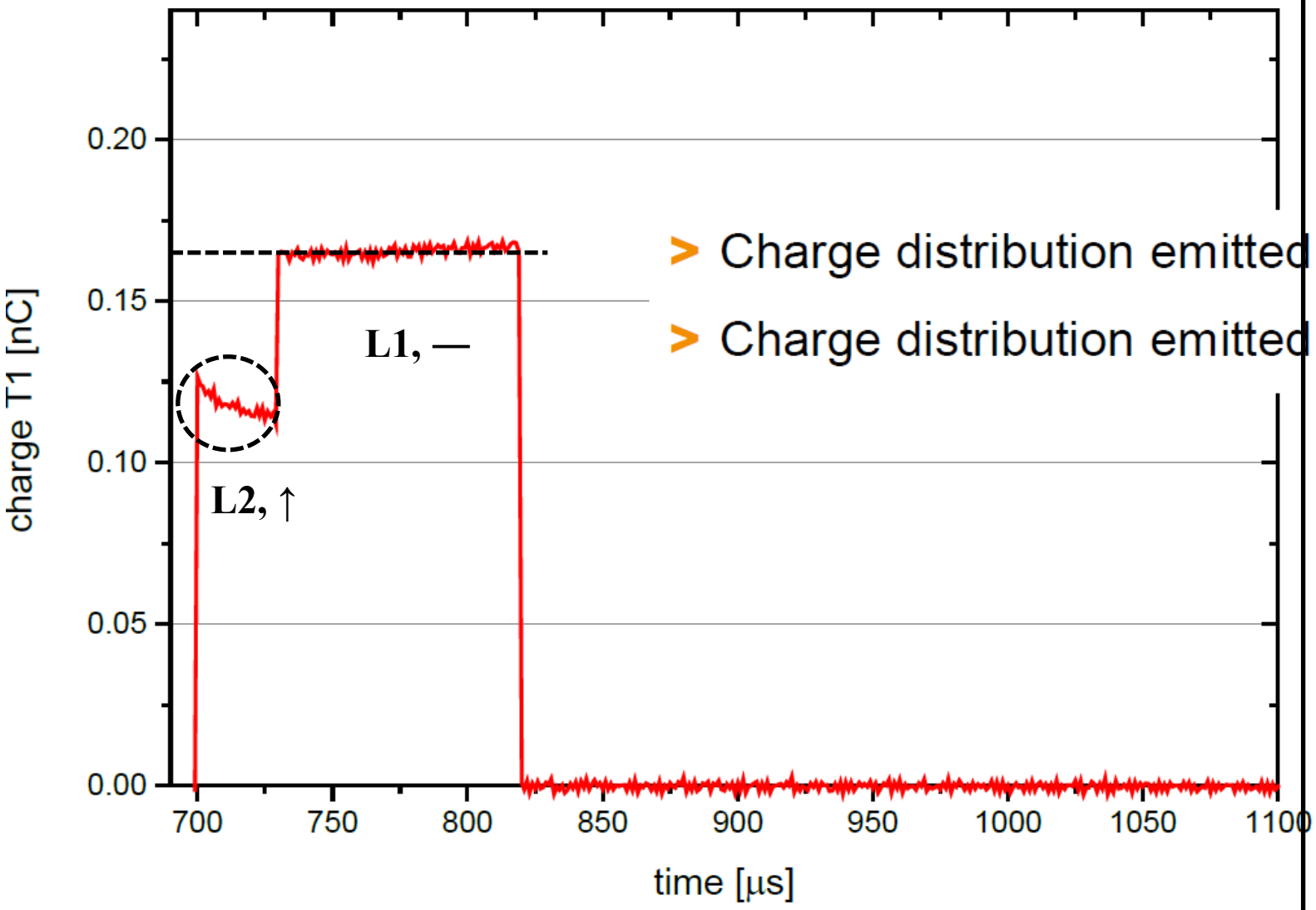

1. Increasing L2 intensity producing much more electrons at the cath. surface, leading to modifications of the local band bending potential already during L2 illumination, resulting in a spiky eff. QE along the L2 train
2. The cath. eff. QE by the start of L1 illumination is reduced compared to that by the start of L2 illumination, due to the local band structure has been flattened to a large extent during L2 illumination (spike decays → QE decays)
3. The L1 illumination with higher intensity tends to further reduce the cath. eff. QE based on the same mechanism, however, an almost-flattened band structure resulted from B.2 not allowing further QE reduction, therefore delivering a flat L1 Q-train

C. L1 and L2 both on cathode, keep L1 intensity, increase L2 intensity step by step

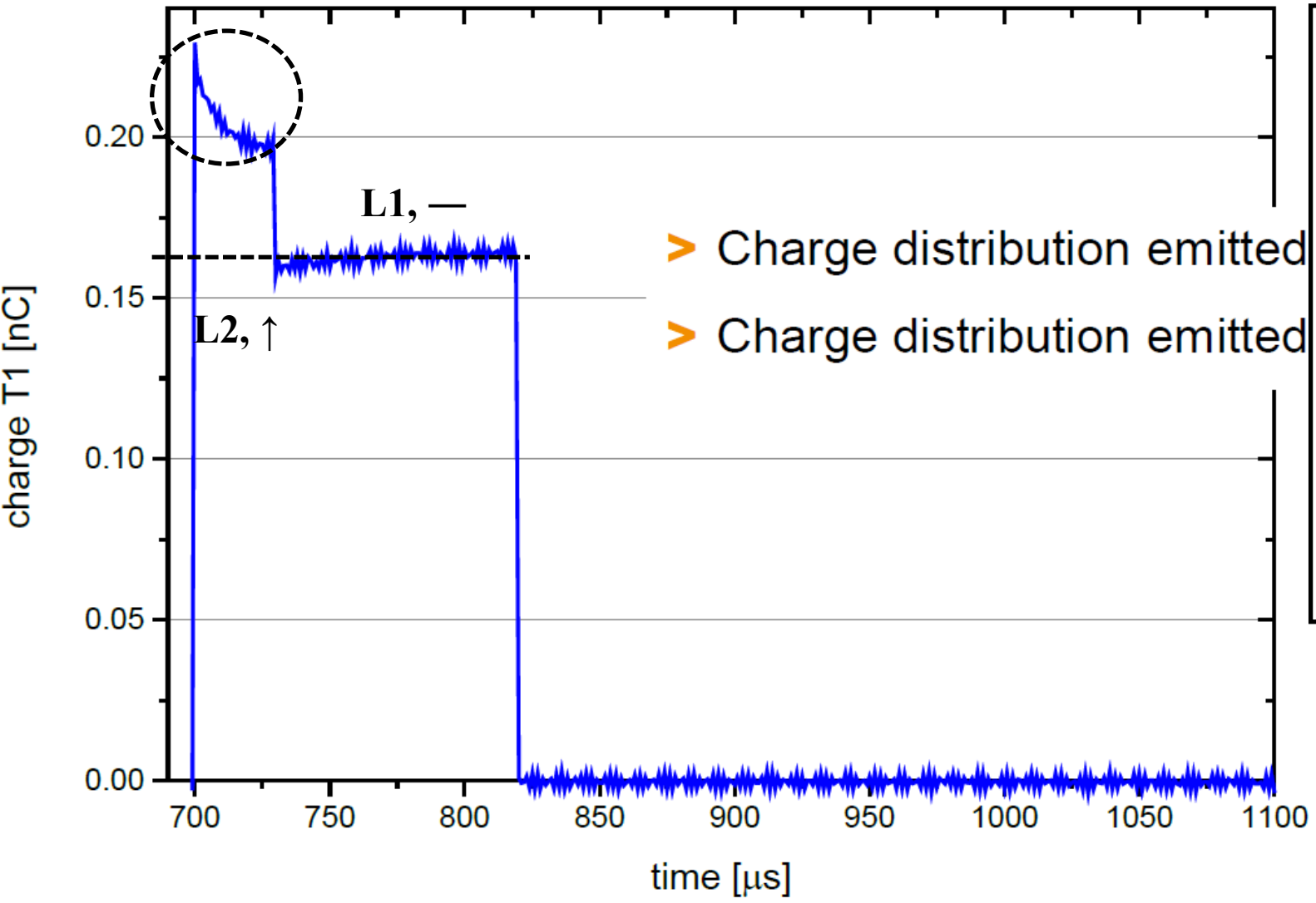

1. Further increasing L2 intensity increases electron production rate at the cath. surface, which influences temporal profile of the spike decaying tendency for a given dopant supplementing rate. Therefore, the temporal profiles of the spikes may be slightly different, but essentially induced by the same mechanism
2. An almost-flat L1 Q-train produced afterwards following B. 3

D. L1 on cathode (w/ RF), L2 off (w/o RF), RF starts from somewhere between L2 and L1

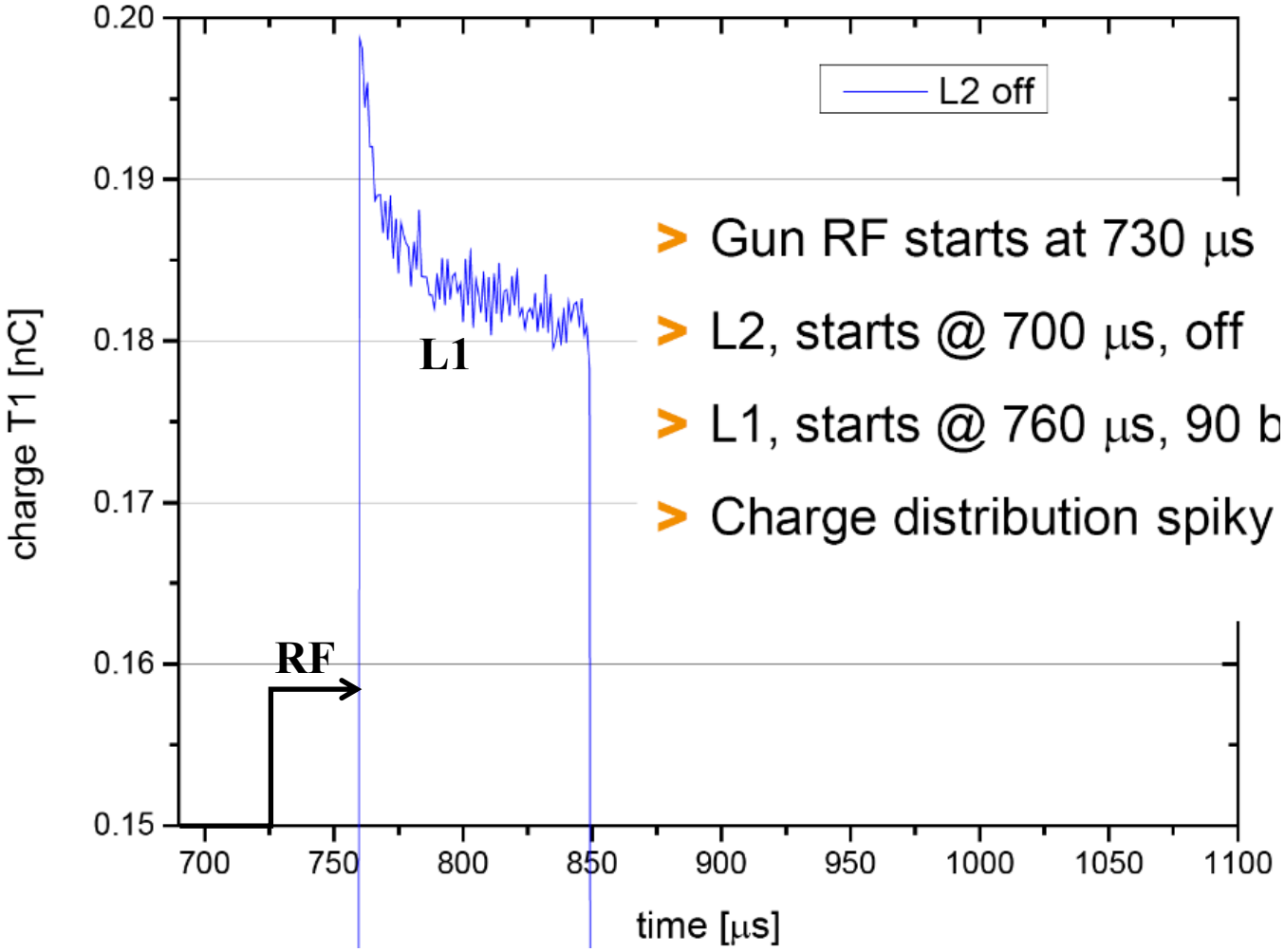

1. L2 off

→ No electrons produced at cath. surface during L2 illumination;

→ No electron local accumulation on the cath. surface either

2. Upon arrival of the L1-train, a big spiky train structure is produced with the presence of L1 and RF, following the same mechanism in **A**, **B** and **C**

E. L1 on cathode (w/ RF), L2 on cathode (w/o RF), RF starts from somewhere between L2 and L1

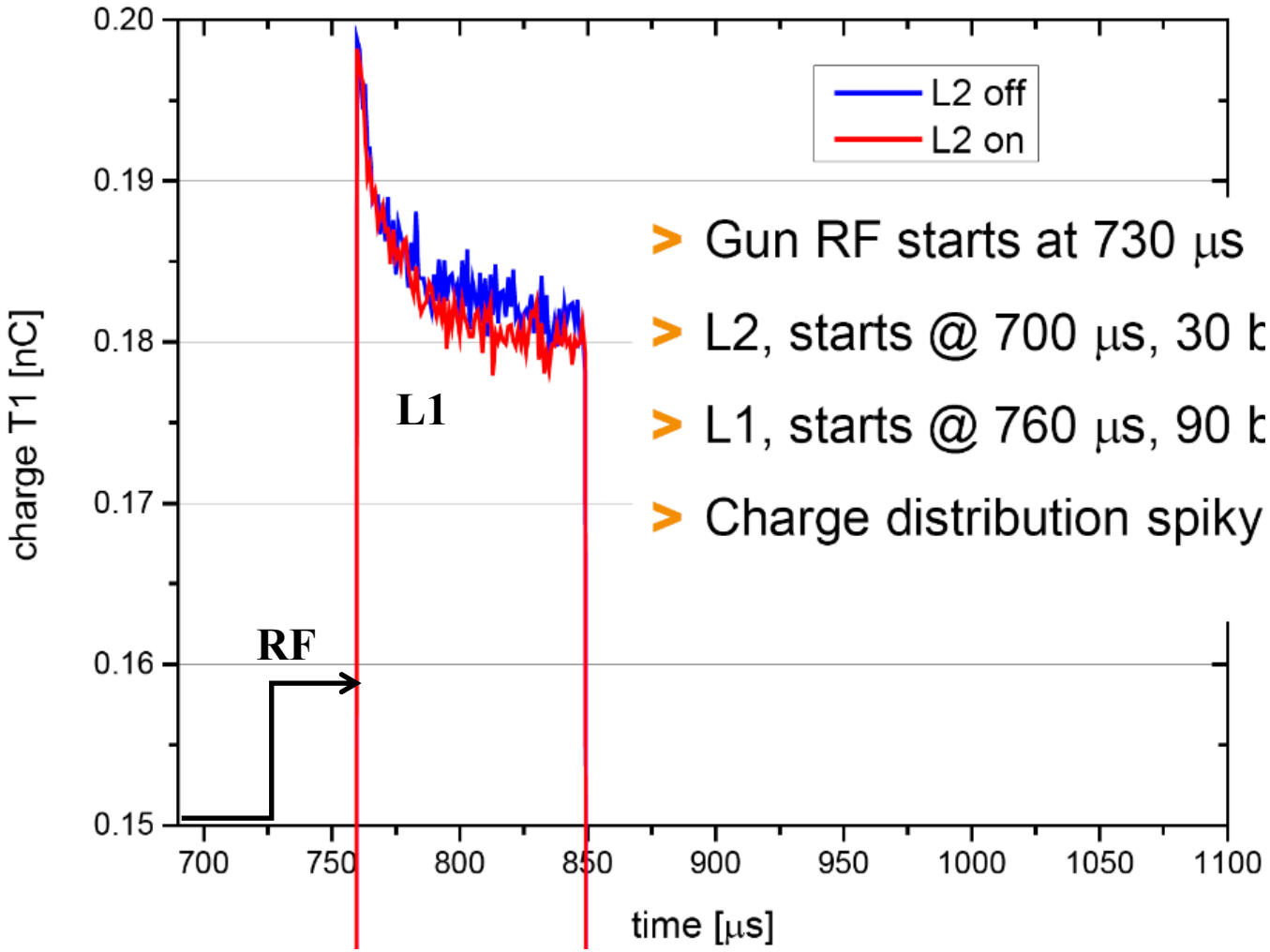

1. L2 on/off, no RF

a. Electron produced during L2 illumination, but no RF seen by the electrons

b. Most produced electrons can not be efficiently extracted to the cath. surface area without RF

c. Switching on and off L2 without RF presence thus not making an obvious impact to the L1 train

d. A slight lower overall cath. eff. QE when L2 on (red) can result from a minority of high energy electrons transported to the cath. surface reducing the band bending level

F. L1 on cathode (w/ RF), L2 on cathode (w/ and w/o RF)

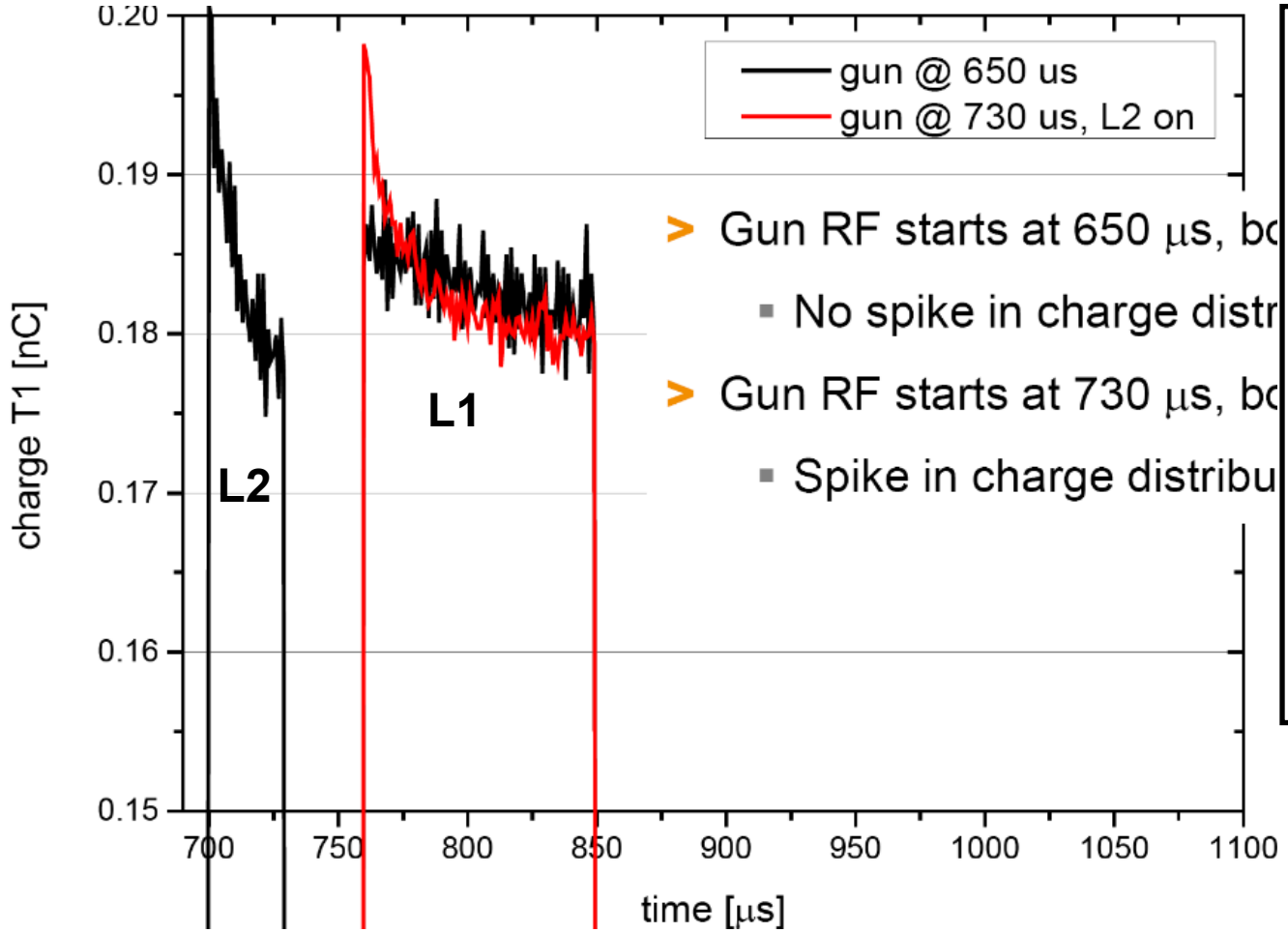

1. L2 on, without RF (red)

→ Following the same mechanism as in **E**

2. L2 on, with RF (black)

→ Impact of the L2 train to the L1 train similar to **A**, **B** and **C**

→ The difference compared to **C** is that there exist some time delays between L2 and L1, using which time the dopant consumption is more supplemented, the flattened band during L2 illumination is again bended to some extent , allowing a slightly increased cath. eff. QE by the start of the L1 train and a weakened decaying tendency afterwards

G. L1 and L2 on cathode (w/ RF), RF power levels adjusted

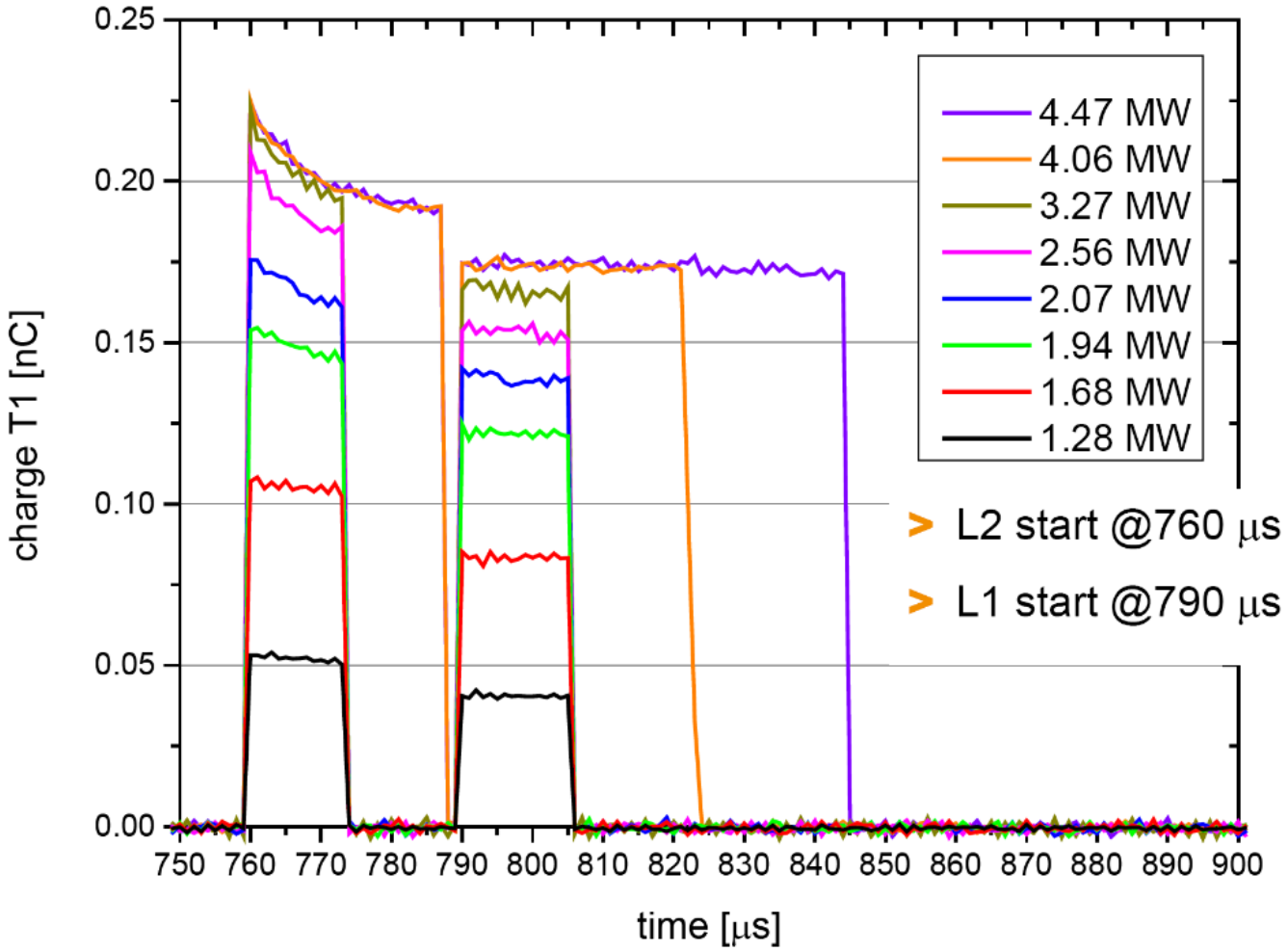

1. Given the intensities of L1 and L2, the charge extraction is reduced with the decrease of the RF power, indicating strong space charge smearing out effect for low RF power levels
2. When RF power is sufficient to extract the produced charges (i.e., 4.47MW and 4.06MW), the spikes during L2 illumination and the flat bunch trains during L1 illumination are perfectly consistent;
3. The mechanism is also consistent to **A**, **B** and **C**

H. L1 and L2 on cathode (w/ RF @ low level), L2 intensity adjusted

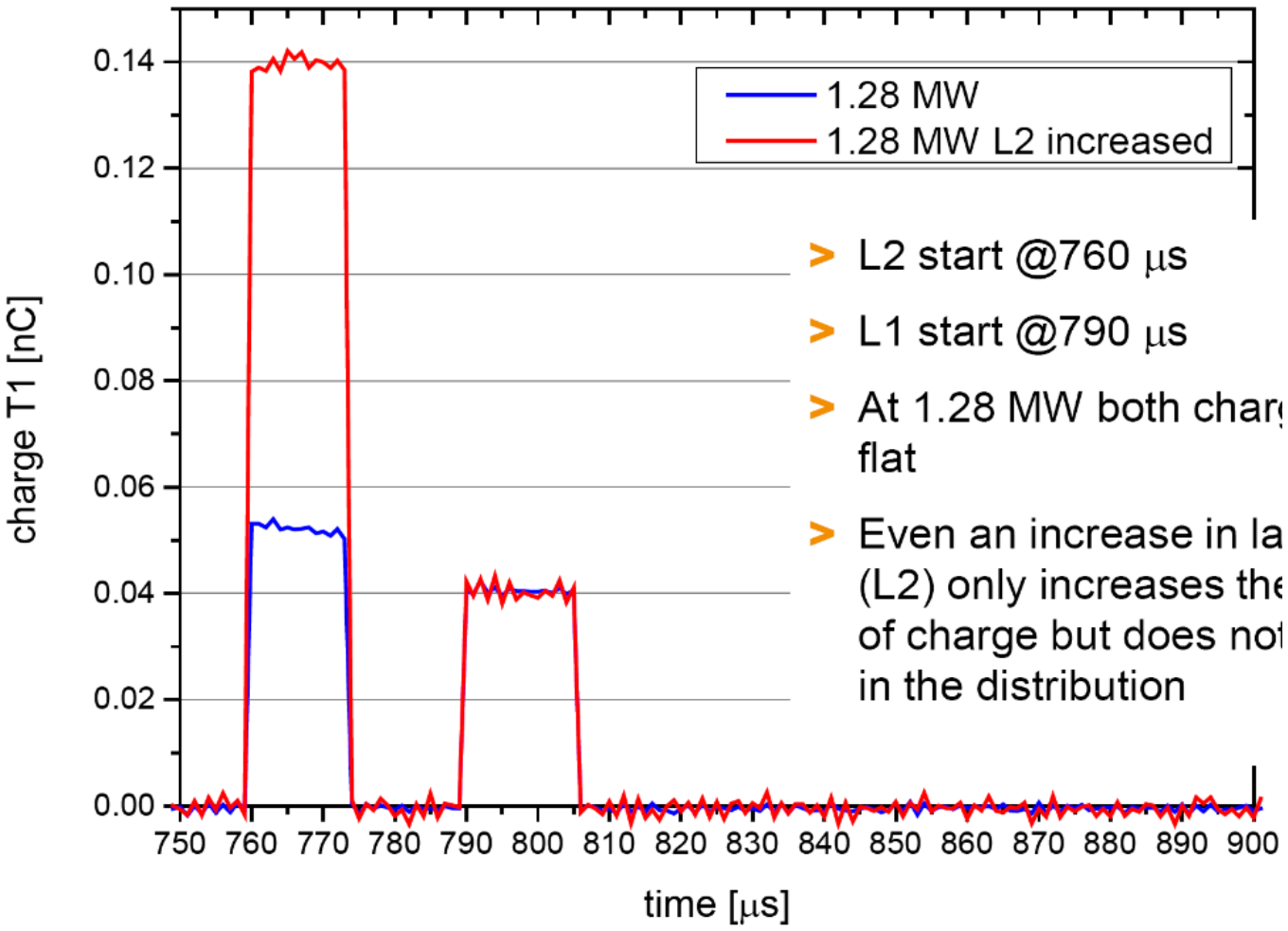

1. Flat Q-train at low RF power level → space charge smearing out effect
2. Increasing L2 intensity can increase the total produced charges during L2 illumination (charge vs. laser energy, even at the "space charge limit")
3. With the same RF power for charge extraction, the emitted bunch still experiences space charge smearing out effect which suppresses the spiky structure showing up

I. L1 and L2 on cathode (w/ RF), L1 delayed w.r.t. L2

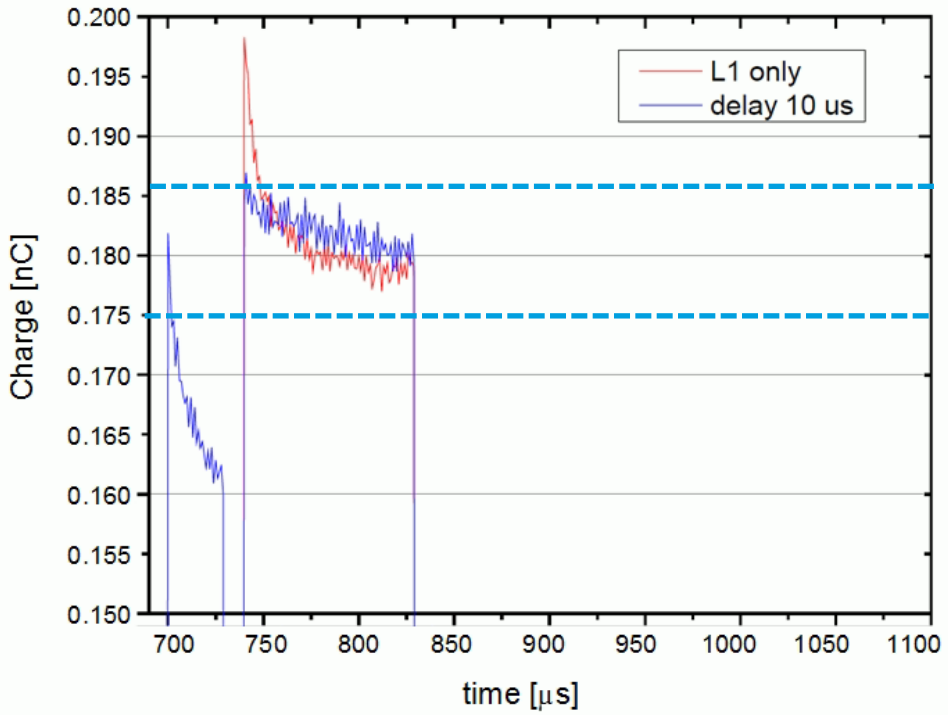

- **L2 and L1 on cathode**
- **L2 30 bunches, start @700 µs**
- **L1 90 bunches, start @730 µs**

1. **If L2 on cathode, the spike in the L1 train is much reduced compared to the case with only L1 on cathode while L2 off** → band bending level largely flattened already during L2 illumination, cath. eff. QE dropping since the start of L2

2. **Increasing the time-delay of L1 w.r.t. L2 →**

   a. Temporal profile of the L1 spike (blue) dynamically varying within the range of ~[0.175, 0.185] nC → due to the presence of L2 illumination the hole consumption on the cath. surface could not be supplemented for an absolute compensation →cath. eff. QE cannot be fully recovered

   b. The temporal profile of the L1 spike (blue) slowly evolving , in a trend of closer shape to the profile (red) when L2 off, as increasing the time delay → insufficient time delay not allowing full QE recovery but longer time delay does impact the flattening rate of the band during L1 (given a fixed intensity) illumination

Other notes

- There may exist other effects which can contribute as well, but with less priorities

→ **Reflectivity change** due to local temperature-increase based optical properties modification

→ discussed with Sven during the last PITZ collaboration meeting

→ temperature effect may be not significant in our case ($\Delta T << \sim 100$ K)

→ **Following-up: thermal effect and/or long living electronic states** based on the paper of C. P. Maag, FEL 2017

→ thermal analysis here done on a time scale of **hundreds nanoseconds** (as it usually is) after an offset subtracted already from the measurement signal in Fig. 2 of the paper (afterwards shown in Fig. 3)

→ excitation of long living states believed to be the reason for the long signal decaying time in Fig. 2, which is theoretically possible for certain type of diamonds (e.g., "type 1b", but this type is not quite commonly presence)